ON FEATURES OF A METHOD FOR THE SUPERFLUIDITY INVESTIGATION AT NUCLEAR EXCITATIONS BELOW THE NEUTRON BINDING ENERGY

Sukhovoj A.M.[1], Mitsyna L.V.[1], Vu D.C.[1, 2], Anh N.N.[3], Hai N.X.[3], Khang P.D.[4], Thang H.H.[3]

[1]*Joint Institute for Nuclear Research, Dubna, 141980, Russia*
[2]*Vietnam Academy of Science and Technology Institute of Physics, Hanoi, Vietnam*
[3]*Dalat Nuclear Research Institute, Vietnam Atomic Energy Institute, Hanoi, Vietnam*
[4]*Hanoi University of Science and Technology, 1 Daicoviet, Hanoi, Vietnam*

Abstract. A simultaneous determination of the nuclear level density (NLD) and the radiative γ-ray strength functions (RSF) is a way to investigate the nuclear superfluidity. The empirical method, proposed for this purpose, is based on analysis of the two-step γ-ray cascades (TSC), which are resulted from a capture of thermal neutrons. At that, different valid assumptions and phenomenological representations of NLD and RSF parameterizations were used and tested for the experimental TSC intensities description. Investigation of 44 nuclei with masses in the region $28 \le A \le 200$ showed an influence of the nuclear shape on the dynamics of a change of a phase of nuclear matter.

1. Introduction

By analogy with the superfluidity effect in metals due to pairing of electrons [1, 2] a pairing of nucleons results in the superfluidity of nuclear matter [3]. As information about pair correlations, thermodynamic characteristics and properties of electromagnetic transitions [4, 5] can be extracted from NLD and RSF values, so in order to understand the process of phase change in nuclear matter it is necessary to determine these two values experimentally.

As it is impossible to resolve all individual levels and to determine probabilities of transitions between them by available now spectrometers, information on the superfluidity can be obtained from indirect experiments only. The method of TSC measuring has been developed at FLNP JINR [6]. In this method TSC of γ-decay following a thermal neutron capture are recorded, and then their intensities are described by functions of some fitted parameters (chosen for NLD and RSF according to appropriate theoretical representations) at the excitation energies from the ground state to neutron resonance [7].

Up to now, the experiment was carried out on 44 nuclei of mass region $28 \le A \le 200$: ^{28}Al, ^{40}K, ^{52}V, ^{60}Co, ^{64}Cu, ^{71}Ge, ^{74}Ge, ^{114}Cd, ^{118}Sn, ^{124}Te, ^{125}Te, ^{128}I, ^{137}Ba, ^{138}Ba, ^{139}Ba, ^{140}La, ^{150}Sm, ^{156}Gd, ^{158}Gd, ^{160}Tb, ^{163}Dy, ^{164}Dy, ^{165}Dy, ^{166}Ho, ^{168}Er, ^{170}Tm, ^{172}Yb, ^{174}Yb, ^{176}Lu, ^{177}Lu, ^{181}Hf, ^{182}Ta, ^{183}W, ^{184}W, ^{185}W, ^{187}W, ^{188}Os, ^{190}Os, ^{191}Os, ^{192}Ir, ^{193}Os, ^{196}Pt, and ^{198}Au.

TSC is determined by the energies of initial, intermediate and final levels as well as the probabilities of electromagnetic transitions between them. In a small interval ΔE of energies of primary transitions the sum of the intensities of TSC from initial states λ to a group of low-lying final states *f* through intermediate levels *i* is determined by an equation:

$$I_{\gamma\gamma}(E_1 \pm \Delta E/2) = \sum_{\lambda,f}\sum_{i} \frac{\Gamma_{\lambda i}}{\Gamma_{\lambda}} \frac{\Gamma_{if}}{\Gamma_{i}} = \sum_{\lambda,f}\sum_{j} \frac{\Gamma_{\lambda j}}{<\Gamma_{\lambda j}> M_{\lambda j}} n_j \frac{\Gamma_{jf}}{<\Gamma_{jf}> m_{jf}}, \qquad (1)$$

where $n_j = \langle\rho_j\rangle \cdot \Delta E$ is the number of excited levels of the cascades in the ΔE energy bin, $\langle\rho_j\rangle$ is a mean value of NLD in the ΔE energy bin, a sum of the partial widths of the primary transitions $\Sigma_j\Gamma_{\lambda j}$ to $M_{\lambda j}$ intermediate levels is $\langle\Gamma_{\lambda j}\rangle M_{\lambda j}$, and a sum $\Sigma_j\Gamma_{jf}$ for the secondary transition to m_{jf} final levels is $\langle\Gamma_{jf}\rangle m_{jf}$, inasmuch as $\langle\Gamma_{\lambda j}\rangle = \Sigma_j\Gamma_{\lambda j}/M_{\lambda j}$ and $\langle\Gamma_{jf}\rangle = \Sigma_j\Gamma_{jf}/m_{jf}$.

The system of equations (1) is nonlinear and strongly correlated. Its solving (by maximum likelihood method) allows to obtain the NLD and RSF values simultaneously. The required NLD and RSF values, which are expressed as functions $\rho(E_{ex})=\varphi(p_1,p_2\ldots)$ and $\Gamma(E_1)= \psi(q_1,q_2\ldots)$ using different valid representations, can be evaluated from the fits of p_1, p_2, … and q_1, q_2, …. parameters to the experimental intensities for all observed γ-transitions.

Now NLD is commonly represented by Gilbert-Cameron formula [8], what combines the Fermi gas model [9] and the constant temperature model [4], the backshift Fermi gas model (BSFM) [10] or phenomenological version of generalized superfluid model (GSM) [11]. Parameters of these models are founded by fitting to the experimental data of cumulative numbers of low-lying levels and the average distance between neutron resonances [12]. As these data cover only an interval of the excitation energies $E_{ex}<E_d$ (E_d is an upper energy of the region of discrete levels) and energies in the vicinity of B_n (B_n is the neutron binding energy), so calculated by these models NLD values will contain unexpected errors in energy region $E_d < E_{ex} < B_n$. There is a similar problem for phenomenological RSF models, as the Kadmenskij-Markushev-Furman model (KMF) [13] or the generalized Lorentzian model (GLO) [14].

However, calculations using abovementioned models of the NLD and RSF indicate that calculated TSC intensities, ${}^{cal}I_{\gamma\gamma}$, are significantly lower than the experimental TSC intensities, ${}^{exp}I_{\gamma\gamma}$. Average values of ratio ${}^{exp}I_{\gamma\gamma}$ /${}^{cal}I_{\gamma\gamma}$ over 40 nuclei are 1.4–2.6 for different models of NLD and RSF [15]. Moreover, it must be said that a strong correlation between NLD and RSF was not taken into account in these models.

2. Experiment

The TSC method with recording of gamma-quanta coincidences following a thermal neutron capture was described in detail in [6]. The spectrometer includes two semiconductor detectors of high efficiency at face-to-face close geometry. TSC to a group of final levels are observed as a group of peaks in the spectrum of sums of amplitudes of coincident pulses (SACP) (see Figure 1.1). Distortion of TSC because of noise coincidences is inhibited and removed by follows:

- coincident events due to γ-quanta backscattering between the detectors are reduced by lead filters 2.5 g/cm^2 in front of each detector's window;
- coincidences with a small energy of γ-quanta are completely eliminated by the threshold for detectors at 520 keV;
- coincidences due to the Compton scattering and random coincidences are removed at an appropriate background subtraction.

Amplitude's codes of coincident pulses are recorded and processed off-line. This procedure brings the possibility to improve the energy resolution of TSC spectra by the numerical algorithm without a loss of efficiency, which was presented in [16].

In order to obtain the experimental TSC intensities we have to determine efficiency of both detectors in the energy region $0.5 <E_\gamma< 9$ MeV. It was done using areas of full-capture peaks of the single γ-ray spectra, which were recorded from $^{35}Cl(n,\gamma)^{36}Cl$ reaction, and known for them γ-ray intensities [17].

After efficiency correction TSC distributions are obtained. Any intensity distribution of two-step cascades contains only peaks of the full capture of the cascade energy and a noise background with a zero average. A dispersion of a background line is effectively diminished at an increase in the number of events of recording of the total energy of the cascade (see Figure 1.2). Each of TSC spectra includes couples of mirror-symmetrical peaks, their center positions correspond to the energies of primary transition (E_1) and secondary transition (E_2). Areas of these mirror-symmetrical peaks are equal to each other. *FWHM* of all resolved peaks is not more than 2–4 keV.

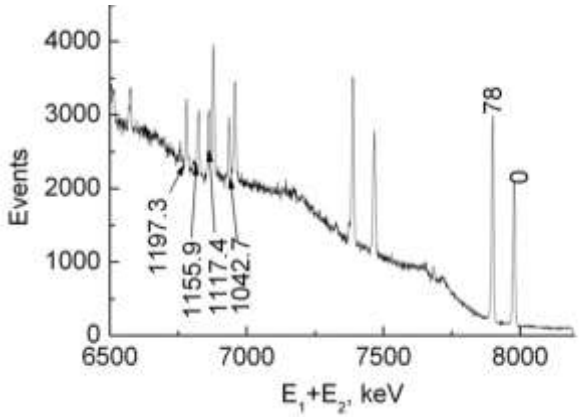

Figure 1.1. A part of SACP spectrum of nucleus ^{172}Yb, the energies of final levels (in keV) of the cascades are written nearby.

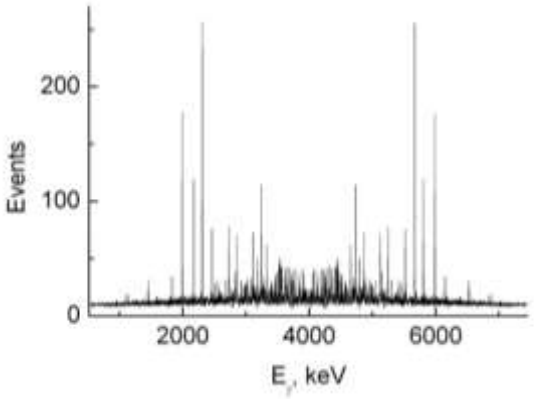

Figure 1.2. The distribution of TSC to the ground state of ^{172}Yb.

Relative intensities $i_{\gamma\gamma}$ of the strongest cascades with intensity i_1 are used for a determination of absolute values of the sum $I_{\gamma\gamma}$ of all cascades: $I_{\gamma\gamma}=i_1 \cdot B_r \cdot 100/i_{\gamma\gamma}$, where the branching ratio B_r is determined from the set of γ-γ coincidences, accumulated in the experiment. And an absolute intensity i_1 (in percent per decay) of primary transitions is usually taken from PGAA [18] or ENDSF [19] files.

3. Determination of the $I_{\gamma\gamma}(E_1)$ distribution

Structure of each TSC spectrum was described in detail in [20], and it consists of three components:

1. a set of pairs of resolved peaks (see Figure 2.1, part A);
2. overlapping distribution of unresolved peaks (Figure 2.1, part B);
3. noise background with zero average line.

Each TSC distribution (as in Figure 1.2) depends on both E_1 and E_2 energies of the cascade quanta. We can consider this distribution as a sum of two mirror-symmetrical distributions, $I_{\gamma\gamma}(E_1)$ and $I_{\gamma\gamma}(E_2)$. For the experimental data analysis by proposed Dubna method it is need to separate $I_{\gamma\gamma}(E_1)$ intensity distribution from the total $I_{\gamma\gamma}(E_1,E_2)$ one. Taking into account that a background is almost absent, an equality of areas of the peaks of primary and secondary transitions (for each individual cascade) and a mirror-symmetry of their positions in relation to the spectrum center at $0.5(E_1+E_2)$, we subtracted all peaks of intense low-energy secondary transitions from the energy interval of the intermediate levels $E_i \geq 0.5B_n$. The rest of intensity in this interval (a continuous distribution of intensity of large number of low-energy primary cascade gamma-quanta) in sum with intense resolved primary transitions from the energy interval $E_i \leq 0.5B_n$ is just the most probable distribution $I_{\gamma\gamma}(E_1)$.

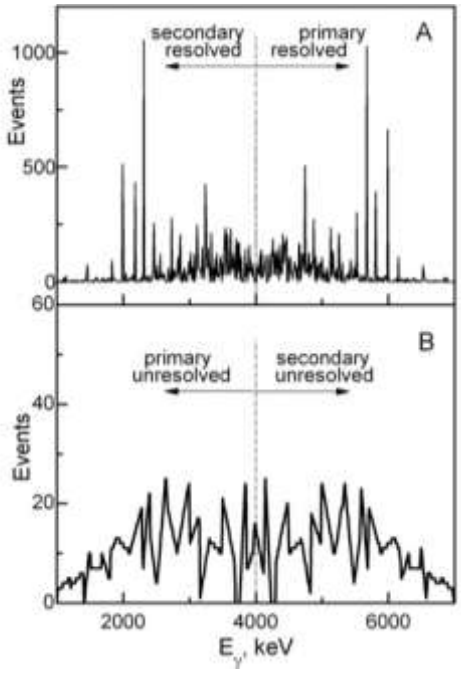

Figure 2.1.Illustration of the $I_{\gamma\gamma}(E_1)$ separation procedure for TSC to the ground state of ^{172}Yb nucleus (the percentage of resolved peaks is 70%).

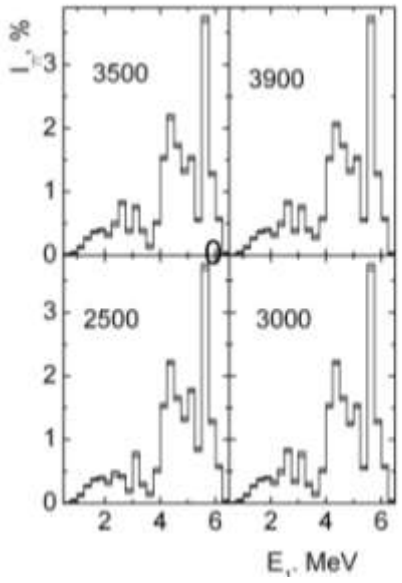

Figure 2.2. Evaluation of the effect of systematic errors for ^{172}Yb in 4 fits at chosen boundary points of "zero primary transitions" at 2500, 3000, 3500, 3900 keV. The spectra were obtained for a sum of intensities of the cascades to the ground state and to the level with E_f = 78 keV.

Of course, if a part of peaks near the energy $0.5(E_1+E_2)$, where there is a mixture of inseparable primary and secondary transitions, is inaccurately identified, the obtained function $I_{\gamma\gamma}= f(E_1)$ distorts. But the part of the intensity of secondary transitions, which are mistakenly included into $I_{\gamma\gamma}(E_1)$, and the part of the intensity of primary transitions, mistakenly included into $I_{\gamma\gamma}(E_2)$, are equal to each other. At that, a possible distortion of a shape of $I_{\gamma\gamma}(E_1)$ distribution in a small energy region of the primary transitions near $0.5B_n$ decreases with an increase in statistics. If TSC are recorded with a sufficient statistic (more than ~ 4000 events at the sum peak), percentage contribution of the unresolved peaks in the total intensity distribution is small. Three of quarter of all investigated nuclei had a minimal required statistic, and it was some times more for the rest of nuclei (in the case of ^{172}Yb, for example, the percentage of resolved TSC to the ground state was 70%). So, a high statistics allows to obtain $I_{\gamma\gamma}(E_1)$ distribution with an accuracy not worse than 10–20% in any energy bins.

In Figure 2.2 the $I_{\gamma\gamma}(E_1)$ distributions are shown, obtained at four chosen boundary points (it is supposed that the intensity of primary transitions decreases to zero in these points): 2500, 3000, 3500 and 3900 keV. As the shape of the $I_{\gamma\gamma}(E_1)$ distribution does not change, so an extension and a shape of the "tail" of unresolved primary transitions, which were taken into account inaccurately, have no influence on the fitting. It means that an uncertainty of such determination of the partial distribution $I_{\gamma\gamma}(E_1)$ is acceptable.

4. The empirical Dubna model

There is a potential for simultaneous estimation of the most probable NLD and RSF values even by model-free method [15] using the Monte-Carlo technique. However, it would be preferable if the NLD and RSF values should be built on a kind of physical assumptions. These assumptions have to take into account shell effects, pairing correlations, collective phenomena of NLD, and also a dependence of width giant dipole resonance on temperature.

The presence of the step-like structure at the fitted NLD curves (this structure was noticed even in [15]) confirms a validity of the superfluid nucleus theory, which interprets the step-like structure as the consequence of breaking Cooper pairs. In the RIPL projects [12] the GSM [11] model has also been considered as a preeminent model. But the GSM model needs in more precise description of the level density below a point of the phase transition.

Description of the NLD function

For a description of the nuclear level density in the empirical Dubna model [21,22] the representations were used:

1) Gaussian distribution $G_n(J)$ for the J-spin-dependent expansion of NLD,
2) a dependence on excitation energy of $\Omega_n(E_{\rm ex})$density ofn-quasi-particle states[23] in the nucleus,
3) a modified (see [24]) phenomenological coefficient $C_{\rm coll}$ [12] for collective effects included the effect of an enhancement of the level density due to vibrational and rotational (for deformed nuclei) excitations.

So, the NLD function was expressed as $\rho(\mathrm{E_{ex}}) = G_n(J) \times \Omega_n(E_{\rm ex}) \times C_{\rm coll}$. The fitted parameters, included in the NLD function $\rho(\mathrm{E_{ex}})=\varphi(U_l,g,A_l,\beta,E_u)$, are: the breaking thresholds U_l (l is a number of Cooper pair) from both $\Omega_n(E_{\rm ex})$ and $C_{\rm coll}$ distributions, the density of single-particle states g near the Fermi-surface from $\Omega_n(E_{\rm ex})$distribution and also parameters of density of vibrational levels A_l above each breaking point, the nuclear deformed parameter β and a rate $E_u$of a change in densities of quasi-particle and phonon levels from $C_{\rm coll}$.

The shell inhomogeneities of a single-particle spectrum were taken into account (as in [24]) through a dependence on excitation energy of the parameters $g=6\cdot a(\mathrm{E_{ex}})/\pi^2$, where $a(\mathrm{E_{ex}})$ is described in detail in [13].

Description of the RSF function

RSF functions both for E1- and M1-transitions are predicted by the model [13] to be smooth, the analysis of the experimental database showed an absolute necessity of an addition of one or two peaks to the smooth parts of them for the better description of TSC intensities [25].

In the Dubna model RSF functions of E1- and M1-transitons are presented by the smooth parts from KMF model [13] in a sum with one or two peaks, each of which is described by asymmetrical Lorentzian curve.

Parameters of the RSF functions (normalized parameter w for the total radiative width Γ_γ, a parameter κ for a possible change of the thermodynamic temperature and also position, width, amplitude and asymmetric parameter of each local i-th peak [24]) of E1- and M1-transitons are fitted separately.

5. The results and discussion

The results of the best $I_{\gamma\gamma}(E_1)$ fits of the radiative widths and the level densities for 43 investigated nuclei are presented in [24] in comparison with their calculations using generally accepted models. In Fig.4 there is an example of $I_{\gamma\gamma}(E_1)$ description for the ^{172}Yb nucleus.

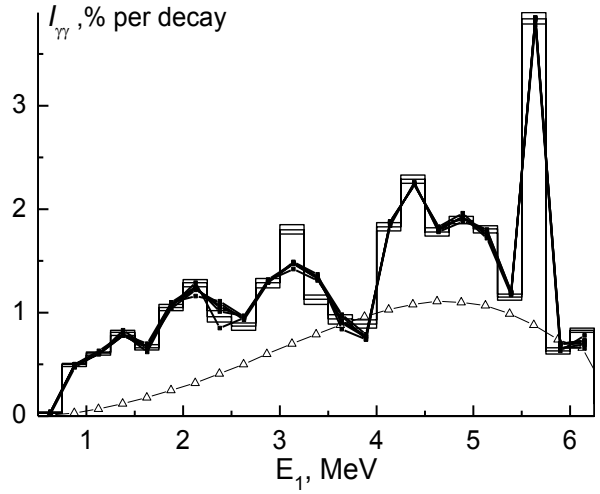

Figure 4.1. The $I_{\gamma\gamma}(E_1)$ distribution for the ^{172}Yb nucleus. Histogram is the experiment with its errors. Broken lines are the results of 5 the best fits. Triangles are the cascade intensity calculated using models [11] and [10].

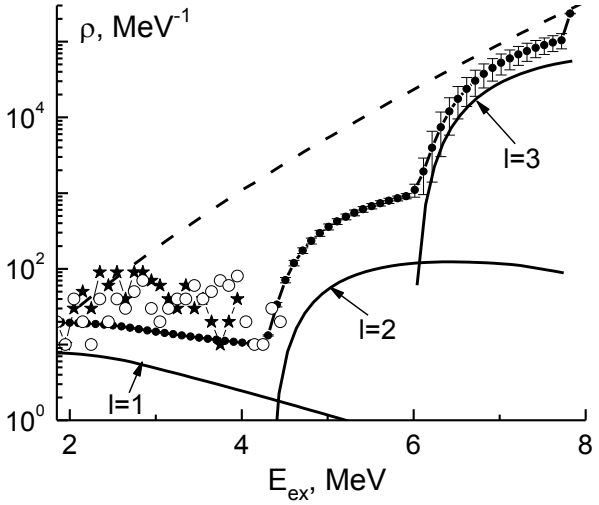

Figure 4.2. Dependence of the level density for ^{172}Yb on the excitation energy. Dased line is the level density predicted by the model [10] for spins $0 \le J \le 3$ and both parities; open points and stars are numbers of "discrete" levels obtained by TSC method and other experiment [26] corresponding; black points with errors are the densities from the best fits to the experimental cascade intensities; solid lines noted by numbers are densities of vibrational levels above the breaking thresholds of 3 Cooper pairs, calculated with fitted parameters.

Using fitted parameters, the NLD and RSF values are simultaneously determined with help of the presented empirical model. Obtained distributions of the NLD for ^{172}Yb nucleus are shown in Figure 5, as an example. For ^{172}Yb, as for all investigated nuclei, the $\rho(E_{ex})$ distributions have a step-wise structure. At the first step (it is usually at excitation energies from 1–2 to 3–4 MeV), above the first breaking point, NLD distribution is mostly constant and is even lowered with an increase of excitation energy (see Figure 5). And energy dependences of NLD above breaking points of the second and the third Cooper pairs rapidly increase as it was predicted by the model [23].

The NLD dependencies on the excitation energy obtained from the Dubna model were compared with ones of the BSFG model, which is considered as a standard model for NLD description in low-energy region and nearby B_n. The comparison showed an agreement between the results in the area near the breaking point of the first Cooper pair and B_n, but at an increase of excitation energy there is a strong divergence between the results of the compared models. However, a plateau, or even a little fall of NLD distributions of Dubna model in the region of excitation energies of 2 – 4 MeV is not in discrepancy with the density of discrete levels obtained from some different experiments (see Figure 5).

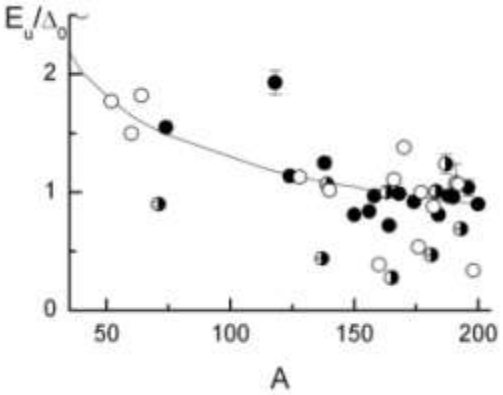

Figure 6. Mass dependencies of E_u fitted parameter for even-even nuclei (black points), even-odd nuclei (half-black points) and odd-odd compound- nuclei (open points).

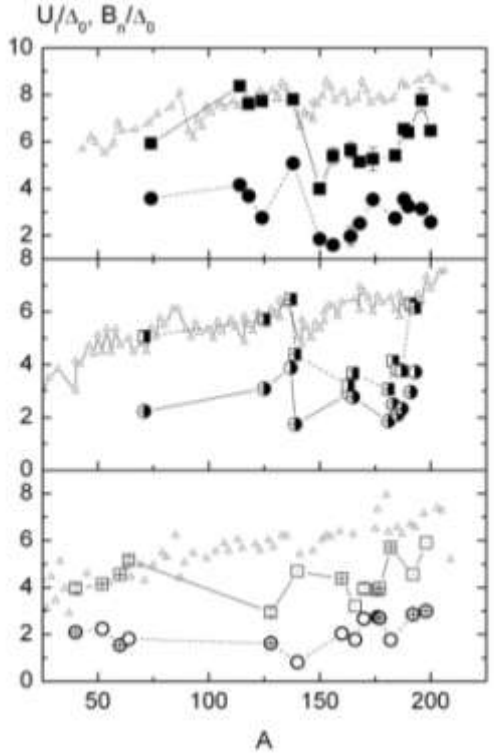

Figure 7. Mass dependencies of breaking thresholds of the second (points) and of the third (squares) Cooper pairs for even-even nuclei (black points), even-odd nuclei (half-black points) and odd-odd compound- nuclei (open points). Triangles are mass dependencies of B_n/Δ_0.

In Figures 6, 7 the mass dependences of fitted parameters for the investigated nuclei are shown: E_u/Δ_0 ratios ($\Delta_0=12.8\cdot A^{1/2}$ is the mean pairing energy of the last nucleon in the nucleus) as well asthe breaking thresholds of the second and of the third Cooper pairs. It is seen that the mean value of E_u/Δ_0 ratios was approximately 1 for about 30 nuclei, and the breaking thresholds of Cooper pairs for spherical nuclei ($A<150$) have values higher than those for deformed nuclei (see Figure 7). It is obvious that for spherical nuclei the breaking thresholds of the 3-rd Cooper pair are about B_n, and for deformed nuclei they are far less.

5. Conclusions

The Dubna empirical model has an ability to describe the experimental $I_{\gamma\gamma}(E_1)$ distributions with a high accuracy. The experimental intensity distributions were measured for 44 nuclei

precisely enough to assert that in case under consideration of the used phenomenological representations the obtained results are reliable:

- ✓ an existence of the superfluid phase of nuclear matter was established at an observation of the behavior of the NLD dependences on the excitation energy during the phase transition process;
- ✓ it was obtained that the energies of the breaking thresholds of Cooper pairs in spherical nuclei are larger than ones for deformed nuclei, i.e. the dynamics of the phase transition in the nuclear matter depends on a shape and a parity of the nucleus.

In order to obtain a more detailed picture of the dynamics of a transition between the fermion and the boson states in the nucleus one should to expand the number of the studied nuclei.

A validity of obtained results depends also on a reliability of the used phenomenological descriptions of NLD and RSF functions, so model evolution is necessary. And, first of all, a replacement of the phenomenological coefficient of enhancement of collective levels by a modern appropriate model must be done.

REFERENCES

1. J. Bardeen, L.N. Cooper, and J.R. Schrieffer, Phys. Rev. **108** (1957)1175.
2. N.N. Bogolyubov, Zh. Ehksp. Teor. Fiz. **34**, 58(1958); Usp. Fiz. Nauk. **67** (1959)549.
3. V.G. Solov'ev, Zh. Ehksp. Teor. Fiz. **36** (1959)1869.
4. T. Ericson, Adv. Phys. **9** (1960)425.
5. J. M. Blatt and V. F. Weisskopf, *Theoretical Nuclear Physics* (Wiley, New York, 1952).
6. S.T. Boneva, É.V. Vasil'eva, Y.P. Popov, A.M. Sukhovoi, and V.A. Khitrov, Sov. J. Part. Nucl. **22** (1991)232.
7. S.T. Boneva *et al.*, Sov. J. Part. Nucl. **22** (1991)698.
8. Gilbert and A.G.W. Cameron, Can. J. Phys. **43** (1965)1446.
9. H. Bethe, Rev. Mod. Phys. **9** (1937)69.
10. W. Dilg, W. Schantl, H. Vonach, and M. Uhl, Nucl. Phys. **A217** (1973)269.
11. A.V. Ignatyuk, *Statistical Properties of Excited Atomic Nuclei* (in Russian). Energoatomizdat, Moscow 1983); Translated by IAEA, Report INDC-233(L) (IAEA Vienna 1985).
12. *Reference Input Parameter Library RIPL-2, Handbook for calculations of nuclear reaction data*, IAEA-TECDOC (2002).
13. S.G. Kadmenskij, V.P. Markushev, and V.I. Furman, Yad. Fiz. **37** (1983)277 [Sov. J. Nucl. Phys. **37** (1983)165].
14. J. Kopecky and R. E. Chrien, Nucl. Phys. **A468** (1987)285.
15. E.V. Vasilieva, A.M. Sukhovoj, V.A. Khitrov, Nucl. Phys. At. Nucl. **64** (2001)153.
16. A.M. Sukhovoj, V.A. Khitrov, Instrum. Exp. Tech. **27** (1984)1071.
17. B. Krusche, K.P. Lieb, H. Daniel et al., Nucl. Phys. **A386** (1982)245.
18. http://www-pub.iaea.org/MTCD/publications/PDF/Pub1263_web.pdf
19. http://www-nds.iaea.org/ENDSF
20. S.T. Boneva, V.A. Khitrov, A.M. Sukhovoj, and A.V. Vojnov, Nucl. Phys. **A589** (1995)293.
21. A.M. Sukhovoj, Phys. Atom. Nucl. **78** (2015)230.
22. L.V. Mitsyna, A.M. Sukhovoj, in Proc. XXII International Seminar on Interaction of Neutrons with Nuclei, Dubna, Russia, May 27-30, 2014 , Preprint № E3-2015-13 (JINR Dubna 2015) p. 245; http://isinn.jinr.ru/past-isinns.html.
23. V.M. Strutinsky, in Proc. International Congress on Nucl. Physics, Paris, France, 1958, p.617.
24. D.C. Vu *et al.*, Phys. Atom. Nucl. **80** (2017)237.
25. A.M. Sukhovoj, V.A. Khitrov, W.I. Furman, Phys. Atom. Nucl. **71** (2008)982.
26. R.C. Greenwood, C.W. Reich, and S.H. Egors, Jr., Nucl. Phys. **262** (1975)260.